1-1-2002

Methylglyoxal Enhances Cisplatin-Induced Cytotoxicity By Activating PKCd

Jonathan P. Godbout

James J. Pesavento
University of Illinois at Urbana-Champaign, jjp6@stmarys-ca.edu

additional author(s)

THE JOURNAL OF BIOLOGICAL CHEMISTRY
Vol. 277, No. 4, Issue of January 25, pp. 2554–2561, 2002
Printed in U.S.A.

Methylglyoxal Enhances Cisplatin-induced Cytotoxicity by Activating Protein Kinase Cδ*

Received for publication, January 16, 2001, and in revised form, September 27, 2001
Published, JBC Papers in Press, November 13, 2001, DOI 10.1074/jbc.M100385200

Jonathan P. Godbout, James Pesavento, Matthew E. Hartman, Scott R. Manson, and Gregory G. Freund‡

From the Departments of Pathology and Animal Sciences, University of Illinois at Urbana-Champaign, Urbana, Illinois 61801

The cytotoxic side effects of anti-neoplastic drugs are increased in patients with either type 1 or type 2 diabetes mellitus by a mechanism that is not clearly defined. We report that the circulating glucose metabolite, methylglyoxal (MGO), enhances cisplatin-induced apoptosis by activating protein kinase Cδ (PKCδ). We found that treatment of myeloma cells with the antioxidant *N*-acetylcysteine completely blocked cisplatin-dependent intracellular GSH oxidation, reactive oxygen species (ROS) generation, poly(ADP-ribose) polymerase cleavage, and apoptosis. Importantly, co-treatment of cells with the reactive carbonyl MGO and cisplatin increased apoptosis by 90% over the expected additive effect of combined MGO and cisplatin treatment. This same synergism was also observed when ROS generation was examined. MGO and cisplatin increased PKCδ activity by 4-fold, and this effect was blocked by the PKCδ inhibitor rottlerin but not by NAC. Furthermore, rottlerin blocked combined MGO and cisplatin-induced ROS generation and apoptosis. Finally, MGO and cisplatin induced c-Abl activation and c-Abl:PKCδ association. Rottlerin blocked c-Abl activation, but the c-Abl inhibitor STI-571 increased MGO and cisplatin-induced apoptosis by 50%. Taken together these data indicate that MGO synergistically enhances cisplatin-induced apoptosis through activation of PKCδ and that PKCδ is critical to both cell death and cell survival pathways. These findings suggest that in the patient with diabetes mellitus heightened oxidative stress can enhance the cytotoxicity of agents that induce DNA damage.

Impaired glucose metabolism and hyperglycemia are critical to the development and pathogenesis of the complications associated with type 1 and type 2 diabetes mellitus (DM)[1] (1). One of these important complications is increased susceptibility to therapeutic drug side effects including those that induce nausea, anorexia, glucose intolerance, neurotoxicity, and nephrotoxcity. In the diabetic patient with cancer, these complications often alter approaches to chemotherapy, accelerate cancer progression, and increase morbidity and mortality (2–5). Presently, however, the cellular mechanisms by which DM complicates chemotherapy are not well understood. The Diabetes Control and Complication Trial identified hyperglycemia as a risk factor for the development of DM complications (6). Importantly, hyperglycemia results in increased intracellular and extracellular concentrations of reactive carbonyls (1). Furthermore, these compounds appear to impact significantly on the progression of DM complications (1, 7, 8) by being potent chemical modifiers of proteins and contributing to the formation of advanced glycation end products.

The reactive carbonyl, methylglyoxal (MGO), is increased by 3–5-fold in the blood and tissues of diabetic patients (8) and circulates at a concentration as high as 8 μM (9). Additionally, MGO-derived dilysine imidazoline cross-links and arginine adducts are also markedly increased (1). MGO is predominantly generated by the non-enzymatic degradation of triose phosphate intermediates through fragmentation and removal of phosphate from the phospho-ene-diolate form of glyceraldehyde 3-phosphate and dihydroxyacetone phosphate (10). In hyperglycemia, MGO formation is enhanced due to elevated concentrations of triose phosphate precursors like glucose, fructose, dihydroxyacetone, and D-glyceraldehyde (1, 7). Detoxification of MGO is mainly via the glyoxalase pathway that is present in the cytosol of all mammalian cells (7). This pathway is composed of glyoxalase I and glyoxalase II, which converts MGO to *S*-D-lactoylglutathione and D-lactate in an enzymatic reaction that requires GSH as a co-factor (7).

Platinum-derived chemotherapeutic agents including the parent compound cisplatin (cis-platinum(II)diammine dichloride) are widely used in the treatment of various malignancies including ovarian (11), testicular (12), and bladder (13) cancers. For the diabetic patient, however, platinum-based drugs are used with reservation due to the concern for exacerbating DM-induced peripheral neuronal and renal damage (2–4). Cisplatin causes apoptotic cell death by generating DNA and protein adducts that include DNA-protein cross-links, DNA monoadducts, inter- and intra-strand DNA cross-links, protein-protein cross-links, and protein adducts (14). Importantly, inhibitors of ROS (15) can block cisplatin-induced apoptosis indicating that pathways involved in and/or activated by oxidative stress are critical to cisplatin bioactivity. In fact, increased concentrations of intracellular GSH are found in cells resistant to cisplatin (16), and cisplatin-induced nephrotoxicity can be blunted by

* This work was supported by National Institutes of Health Grant CA-61931 (to G. G. F.), the Macula Foundation, Inc. (to G. G. F.), the American Diabetes Association (to G. G. F. and M. E. H), the American Heart Association (to G. G. F.), and United States Department of Agriculture/Cooperative State Research Education and Extension Service (CSREES), Hatch (to G. G. F.). The costs of publication of this article were defrayed in part by the payment of page charges. This article must therefore be hereby marked "*advertisement*" in accordance with 18 U.S.C. Section 1734 solely to indicate this fact.

‡ To whom correspondence and reprint requests should be addressed: Dept. of Pathology, College of Medicine, 506 South Mathews Avenue, University of Illinois at Urbana Champaign, Urbana, IL 61801. Tel.: 217-244-8839; Fax: 217-244-5617; E-mail: freun@uiuc.edu.

[1] The abbreviations used are: DM, diabetes mellitus; H_2DCF-DA, 5(and 6)-carboxy-2′,7′-dichlorodihydrofluorescein diacetate; MGO, methylglyoxal; MEK, mitogen-activated protein kinase/extracellular signal-regulated kinase kinase; NAC, *N*-acetylcysteine; PARP, poly(ADP-ribose) polymerase; PIK, phosphatidylinositol kinase; PKC, protein kinase C; ROS, reactive oxygen species; Z-Asp, Z-Asp-2,6-dichlorobenzoyloxymethyl ketone; PI, propidium iodide; AMC, 7-amino-4-methylcoumarin.

systemic administration of NAC (17). As expected, depletion of intercellular GSH with GSH synthesis inhibitors increases the cytotoxic effects of cisplatin and correlates with enhanced intracellular production of ROS (15, 18).

PKCδ is implicated as a critical mediator of oxidative and genotoxic stress (19–21). Furthermore, PKCδ activity is elevated in the diabetic patient with hyperglycemia and is believed to play a role in the development of diabetic vascular complications (22). The PKC family is currently composed of at least 10 related isozymes that have been divided into three groups based on their structure and cofactor requirements. The conventional PKC isoforms (cPKC) α, βI, βII, and γ require diacylglyerol, phosphatidylserine, and Ca^{2+} for activity. The novel isoforms δ, ϵ, η, and θ require diacylglyerol and phosphatidylserine but not Ca^{2+} for activity, and the atypical isoforms ζ and ι require only phosphatidylserine for activity (reviewed in Refs. 23–27). Structurally PKCδ is a 78-kDa protein that contains a C-terminal catalytic domain, two conserved regions C2 and C3 essential for activity, a substrate binding domain, and an N-terminal regulatory domain with an inhibitable pseudo-substrate domain and two cysteine-rich zinc fingers (28). In the presence of lipid binding, the pseudo-substrate is liberated from the active site, and PKCδ autophosphorylates and becomes active. Rotterlin, which competitively blocks the ATP-binding site of PKCδ, is a specific inhibitor with an IC_{50} value between 3 and 6 μM (29). Importantly, activation of PKCs has been shown to increase the sensitivity of cells to cisplatin (30, 31). In addition, inhibition of PKCδ activity with rottlerin blocks caspase activation and cisplatin-induced cell death (32). We show that MGO enhances cisplatin-induced apoptosis by activating PKCδ and that PKCδ activation is critical to both cell death and survival.

EXPERIMENTAL PROCEDURES

Materials—The myeloma cell line U266 was purchased from the American Type Culture Collection (Manassas, VA). All cell culture reagents and chemicals were purchased from Sigma except as noted below. Neonate calf serum (0.05 ng/ml, 0.48 enzyme units/ml endotoxin) was purchased from Biocell Laboratories (Rancho Dominguez, CA). [γ-^{32}P]ATP, protein G-Sepharose, and ECL Western blotting Analysis System were purchased from Amersham Biosciences. Hoechst 33342, propidium iodide, and H_2DCF-DA were purchased from Molecular Probes (Eugene, OR). Caspase-3 substrate (Ac-DEVD-AMC) and PD98059 were purchased from Calbiochem. Z-Asp was purchased from Bachem (King of Prussia, PA). Bio-Rad protein reagent was purchased from Bio-Rad. Anti-p53, anti-p21^{Cip}, and anti-c-Abl antibodies were purchased from Upstate Biotechnology, Inc. Anti-PKCδ antibody was purchased from Santa Cruz Biotechnology (Santa Cruz, CA). Anti-phospho-PKCα, -βI, -βII, -γ, and -δ antibodies were purchased from Cell Signaling Technology (Beverly, MA). Nitrocellulose membrane was purchased from Osmotic (Westborough, MA). STI-571 was purchased from Carle Clinic Pharmacy (Urbana, IL).

Apoptosis and Cell Viability by Flow Cytometry Using Hoechst and Propidium Iodide (PI) Double Staining and PI Staining—Flow cytometric evaluation of apoptosis by double staining was performed as previously described (33). In brief, cells were treated as indicated, and after 18 h, 0.9 μg/ml Hoechst 33342 was added to cells at 37 °C for 3 min. PI (6 μg/ml) was then added, and cells were incubated on ice for 5 min. Ten thousand cells were analyzed, and apoptotic cells were identified as those with increased Hoechst fluorescence, low forward angle light scatter, and low PI fluorescence.

Intracellular Peroxides—Flow cytometric detection of intracellular peroxide was performed as previously described (34). For intracellular peroxide measurements, cells were treated as indicated and then loaded with 5 μM H_2DCF-DA for 3 h. Ten thousand cells were analyzed by flow cytometry, and peroxide-containing cells were identified as those with increased fluorescein isothiocyanate fluorescence of oxidized H_2DCF-DA.

Caspase Activity—Caspase activity was assayed as previously described (33). In brief, cells were treated as indicated and then lysed in 1 mM EDTA, 10 mM EGTA, 10 μM digitonin, and 50 mM Tris, pH 7.4, at 37 °C for 15 min. Lysates were clarified by centrifugation and incubated with 50 μM of the caspase-3-specific substrate Ac-DEVD-AMC (35) for 1 h at 37 °C. Fluorescence of released 7-amino-4-methylcoumarin (AMC) was measured at an excitation of 380 nM and an emission of 460 nM.

GSH—GSH was determined as previously described (36). In brief, cells were lysed in 0.2% Triton X-100 and 2.5% sulfosalicylic acid, and total proteins were determined in clarified lysates with the Bio-Rad protein reagent. Total GSH was assayed using a version of Giffith's method (37) monitoring the change of absorbance at 412 nm in the presence of 0.1 mM 5,5′-dithiobis-(2-nitrobenzioc acid), 0.15 mM NADPH, and 1 unit of GSH reductase/ml in a phosphate buffer containing 1 mM EDTA, pH 7.5. GSH concentration was calculated by comparison with an internal GSH standard and expressed as nanograms of GSH equivalents/μg of protein.

Western Analysis—Western analysis was performed as previously described (38). In brief, 15×10^6 cells were lysed in 1 ml of ice-cold 1% Triton X-100, 100 mM NaCl, 50 mM NaF, 1 mM phenylmethylsulfonyl fluoride, 2 μg/ml aprotinin, 2 μg/ml leupeptin, 2 mM sodium orthovanadate, 1 mM dithiothreitol, and 50 mM Tris base, pH 7.4. Proteins were resolved by SDS-PAGE (250 μg/lane) under reducing conditions in 10% gels and then electrotransferred to nitrocellulose. Immunoreactive proteins were visualized using the indicated primary antibodies and ECL reagents followed by autoradiography and densitometry.

PKCδ Kinase Assays—PKCδ assays were performed as previously described (21). In brief, cells were treated as indicated and then lysed in ice-cold 1% Triton X-100, 1 mM EDTA, 1 mM EGTA, 100 mM NaCl, 50 mM NaF, 25 mM benzamidine, 2 mM sodium orthovanadate, 1 mM dithiothreitol, 2 μg/ml leupeptin, 2 μg/ml aprotinin, 1 mM phenylmethylsulfonyl fluoride, and 50 mM Tris, pH 7.4. Lysates were clarified, and PKCδ was immunoprecipitated for 2 h with an anti-PKCδ antibody. Immune complexes were extensively washed and kinase reactions performed at 30 °C in 20 mM Tris-HCl, pH 7.5, with 10 mM $MgCl_2$, 20 μM [γ-^{32}P]ATP (16.7 μCi/nmol), and 200 μg/ml H1 histone. Reactions were terminated after 5 min by addition of 2× SDS-PAGE load buffer and analyzed in 15% acrylamide gels by autoradiography. Autoradiographs were quantified by densitometry.

c-Abl Kinase Assays—c-Abl assays were performed by a modification of a procedure previously described (39). In brief, cells were treated as indicated and then lysed in ice-cold 1% Triton X-100, 1 mM EDTA, 1 mM EGTA, 100 mM NaCl, 50 mM NaF, 25 mM benzamidine, 2 mM sodium orthovanadate, 1 mM dithiothreitol, 2 μg/ml leupeptin, 2 μg/ml aprotinin, 1 mM phenylmethylsulfonyl fluoride, and 50 mM Tris, pH 7.4. Lysates were clarified, and c-Abl was immunoprecipitated for 2 h with an anti-c-Abl antibody. Immune complexes were extensively washed and kinase reactions performed at 30 °C in 20 mM Tris-HCl, pH 7.5, with 10 mM $MnCl_2$, 20 μM [γ-^{32}P]ATP (16.7 μCi/nmol), and 5 μg/ml IRS-1-(511–772). Reactions were terminated after 10 min by addition of 2× SDS-PAGE load buffer and resultant phosphoproteins resolved under reducing conditions in 15% gels. Serine and threonine phosphoamino acids were base-hydrolyzed (38), and phosphotyrosine-containing proteins were analyzed by autoradiography and quantified by densitometry.

Statistical Analysis—Where indicated experimental data were analyzed either by the Student's *t* test for comparison of means using Microsoft Excel (Redmond, WA) or by a two- or three-factor factorial assuming unequal variances using Statistical Analysis Software (Cary, NC).

RESULTS

Timing of Cisplatin-dependent ROS Accumulation and GSH Reduction—ROS accumulation and GSH reduction are critical to the bioactivity of cisplatin (15–18), but the timing of these intracellular changes has not been fully defined. Fig. 1*A* (*left panel*) demonstrates that after 18 h of cisplatin treatment a dose-dependent increase in apoptosis occurred as measured by dual staining with Hoechst and PI. At 1 μg/ml cisplatin, 11.1 ± 1.9% of cells were apoptotic. At 5, 7.5, and 15 μg/ml cisplatin, 32.1 ± 3.3, 50.7 ± 2.5, and 67.4 ± 0.5% of cells were apoptotic. Cells not treated with cisplatin were 3.7 ± 0.3% apoptotic. Fig. 1*A* (*right panel*) shows that the antioxidant NAC reduced cisplatin-dependent apoptosis in a dose-dependent manner. At 0.5 mM NAC, apoptosis was decreased 12% from 68.7 ± 0.9 to 60.5 ± 4.0%. At 1, 5, 10, and 25 mM NAC, apoptosis was reduced 29, 82.4, 91, and 92%, respectively. Untreated cells were 3.7 ± 0.5% apoptotic. To examine further cisplatin-in-

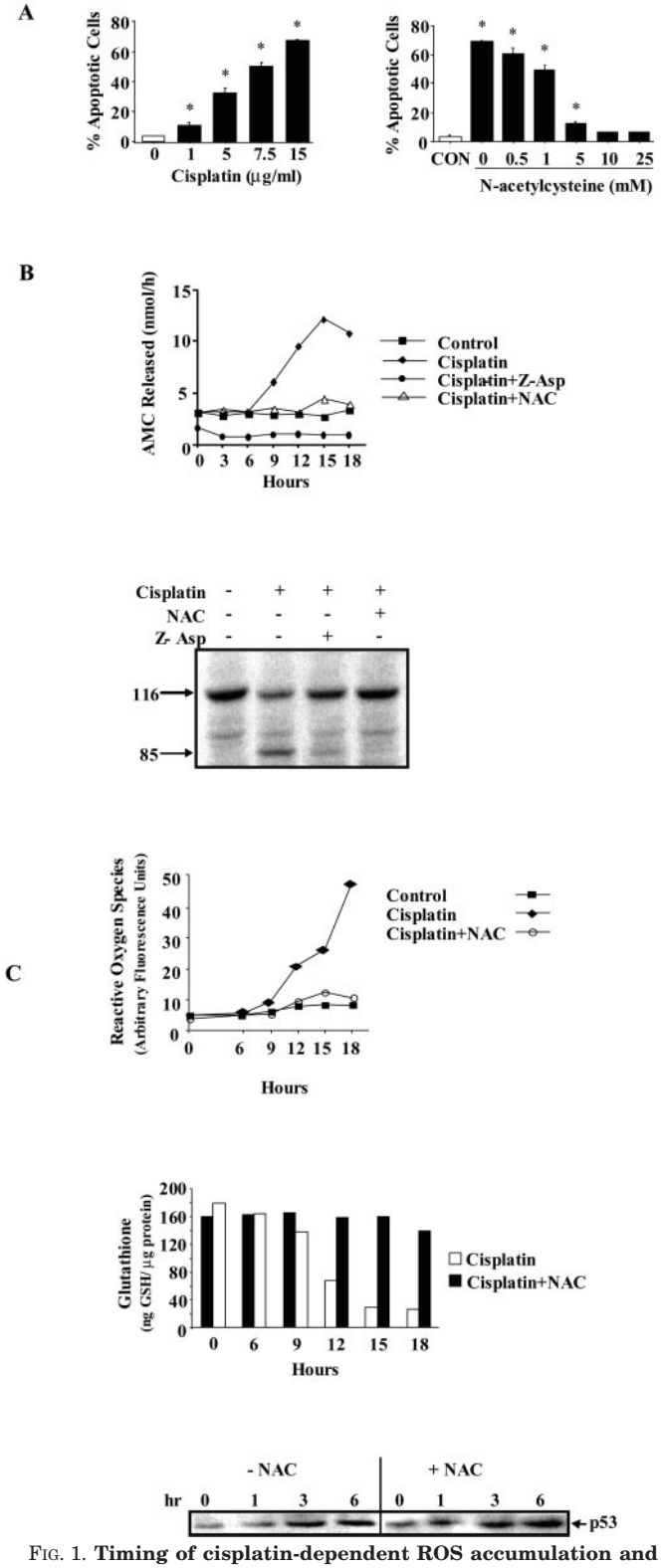

FIG. 1. **Timing of cisplatin-dependent ROS accumulation and GSH reduction.** *A, left panel*, cells were treated with the cisplatin concentrations indicated for 18 h, and apoptotic cell death was measured by flow cytometry using Hoechst and PI double staining. Results represent an average of three independent experiments ± S.E. Results significantly different from 0 at $\alpha = 0.05$ are indicated by *. *A*, *right panel,* cells were treated for 18 h with (*solid bars*) or without (*CON*) 15 μg/ml cisplatin, and the NAC concentrations are indicated (*underline*). Apoptotic cell death was measured by flow cytometry using Hoechst and PI double staining. Results represent an average of three independent experiments ± S.E. Results significantly different from control at $\alpha = 0.05$ are indicated by *. *B, top panel*, cells were treated for the times indicated with or without (control) 15 μg/ml cisplatin and 50 μg/ml Z-Asp. Caspase-3 activity was measured in clarified cell lysates by fluorometry using Ac-DEVD-AMC as a substrate. Results are representative of three independent experiments. *B, bottom panel,* cells were treated for 15 h with or without 15 μg/ml cisplatin, 10 mM NAC, and/or 50 μg/ml Z-Asp as indicated. PARP cleavage was measured by Western analysis of whole cell lysates using an anti-PARP antibody. Results are representative of three independent experiments. *C, top panel,* cells were treated for the times indicated with or without (control) 15 μg/ml cisplatin and 10 mM NAC. ROS were measured by flow cytometry using H_2DCF-DA staining. Results are representative of three independent experiments. *C, middle panel,* cells were treated with 15 μg/ml cisplatin for the indicated times with (*black bars*) or without (*white bars*) 10 mM NAC. Intracellular GSH was determined spectrophotometrically as described under "Experimental Procedures." Results are representative of three independent experiments. *C, bottom panel,* cells were treated as in *C, middle panel,* and p53 mass was measured by Western analysis of whole cell lysates using an anti-p53 antibody. Results are representative of three independent experiments.

duced apoptosis, caspase-3 activation was measured during 15 μg/ml cisplatin treatment. Fig. 1*B* (*top panel*) shows that after cisplatin treatment caspase-3 became activated between 6 and 9 h, and this activity peaked at 4-fold over basal at 15 h. Pretreatment of cells for 15 min with either NAC (10 mM) or the caspase inhibitor Z-Asp (50 μg/ml) blocked cisplatin-induced caspase-3 activation and PARP cleavage (Fig. 1*B, bottom panel*). Because thiol-containing compounds like NAC can block ROS accumulation, we next looked at cisplatin-dependent intracellular ROS accumulation and GSH concentration. Fig. 1*C* (*top panel*) shows that 15 μg/ml cisplatin induced a measurable increase in intracellular peroxide between 6 and 9 h after cisplatin treatment. At 12, 15, and 18 h, cellular peroxide levels increased 2.7-, 3.2-, and 5.8-fold, respectively. Pretreatment of cells for 15 min with 10 mM NAC reduced cisplatin-dependent peroxide generation by 100% at 9 h, 89% at 12 h, 78% at 15 h, and at 93% at 18 h. Fig. 1*C* (*middle panel*) demonstrates that intracellular GSH decreased along a similar time course. After 15 μg/ml cisplatin treatment, the first detectable loss of intracellular GSH occurred between 6 and 9 h and by 18 h GSH was reduced by 8-fold. When cells were pretreated with 10 mM NAC for 15 min, GSH reduction induced by cisplatin was completely blocked, but basal intracellular GSH levels were not significantly affected. Fig. 1*C* (*bottom panel*) shows that NAC pretreatment did not interfere with the early cisplatin-signaling event of increasing p53 mass between 0 and 6 h. Taken together, these findings indicate the following: 1) that cisplatin induces an NAC-inhibitable accumulation of ROS and GSH loss between 6 and 9 h after cisplatin treatment, 2) that blockage of ROS accumulation prevents cisplatin-dependent caspase-3 activation and apoptosis, and 3) that certain early events likely related to DNA damage as in p53 accumulation are unaffected by NAC and its impact on ROS and GSH.

Methylglyoxal Synergizes with Cisplatin to Induce Apoptosis—MGO is a cytotoxic glucose metabolite (1) that requires GSH as a co-factor during its intracellular detoxification (7). To determine whether MGO increased cisplatin cytotoxicity, apoptosis was examined by dual staining with Hoechst and PI. Fig. 2*A* demonstrates that when cells were treated with 3 μg/ml cisplatin for 18 h apoptosis increased from 1.17 ± 0.23 to 18.72 ± 3.6%. When cells were treated concurrently with 5 or 10 μM MGO + 3 μg/ml cisplatin, apoptosis increased to 35.14 ± 6.6 and 46.7 ± 6.46%, respectively. By itself, the apoptosis induced by 5 and 10 μM MGO was 1.31 ± 0.29 and 5.2 ± 2.3%, respectively. Importantly, the apoptosis induced by MGO + cisplatin (18.72 ± 3.6 to 35.14 ± 6.6% and 18.72 ± 3.6 to 46.7 ± 6.46% for 5 and 10 μM MGO + 3 μg/ml cisplatin, respectively) was significantly different at $\alpha = 0.05$ than the additive affects expected (1.31 ± 0.29 + 18.72 ± 3.6%, for 5 μM MGO + cisplatin and 5.2 ± 2.3 + 18.72 ± 3.6% for 10 μM MGO +

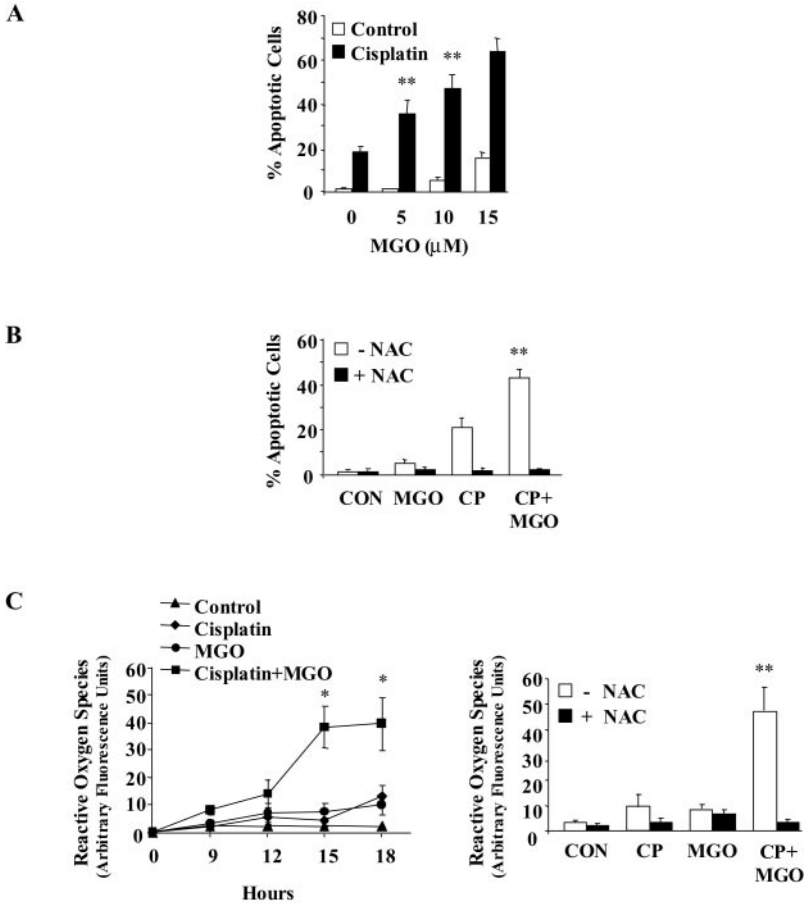

FIG. 2. **Methylglyoxal synergizes with cisplatin to induce apoptosis.** *A,* cells were treated with (*solid bars*) or without (*open bars*) 3 μg/ml cisplatin and the MGO concentrations indicated for 18 h. Apoptotic cell death was measured by flow cytometry using Hoechst and PI double staining. Results represent an average of three independent experiments ± S.E. Results significantly different from 3 μg/ml cisplatin + 0 μM MGO at $\alpha = 0.05$ by a two-factor factorial assuming unequal variances are indicated by **. *B,* cells were treated either with or without (*CON*) 3 μg/ml cisplatin (*CP*), 10 μM MGO, and/or 10 mM NAC as indicated. Apoptotic cell death was measured by flow cytometry using Hoechst and PI double staining. Results represent an average of three independent experiments ± S.E. Results significantly different from CP −NAC at $\alpha = 0.05$ by a three-factor factorial assuming unequal variances are indicated by **. *C, left panel*, cells were treated for 18 h with or without (*CON*) 3 μg/ml cisplatin and/or 10 μM MGO as indicated. ROS accumulation was measured by flow cytometry using H_2DCF-DA staining. Results represent an average of three independent experiments ± S.E. Results significantly different from cisplatin at $\alpha = 0.05$ by a two factor factorial assuming unequal variances are indicated by **. *C, right panel,* cells were treated as in *B,* and ROS accumulation was measured by flow cytometry using H_2DCF-DA staining. Results represent an average of three independent experiments ± S.E. Results significantly different from cisplatin (*CP*) at $\alpha = 0.05$ by a two-factor factorial assuming unequal variances are indicated by **.

cisplatin). Because oxidative stress and GSH play a critical role in the bioactivities of both MGO and cisplatin, the next step was to investigate the combined impact of MGO + cisplatin on these pathways. Fig. 2*B* shows that pretreatment of cells for 15 min with 10 mM NAC completely blocked apoptosis induced by 10 μM MGO + 3 μg/ml cisplatin. Fig. 2*C* (*left panel*) demonstrates that 10 μM MGO + 3 μg/ml cisplatin increased intracellular peroxides by 4-fold at 15 h when compared with cisplatin or MGO alone. Fig. 2*C* (*right panel*) shows that 10 mM NAC pretreatment completely inhibited ROS accumulation at 15 h induced by either 3 μg/ml cisplatin, 10 μM MGO, or 10 μM MGO + 3 μg/ml cisplatin in combination. Taken together, these findings indicate that MGO and cisplatin work in synergy to induce apoptosis by increasing intracellular ROS generation.

Inhibition of PKCδ with Rottlerin Blocks MGO/Cisplatin-dependent Apoptosis and ROS Generation—Inhibition of PKCδ activity with rottlerin has been shown to block cisplatin-dependent apoptosis (32). To determine whether PKCδ was required for MGO/cisplatin-dependent cytotoxicity, flow cytometry was performed. Fig. 3*A* demonstrates that pretreatment of cells with 5 μM rottlerin for 15 min completely blocked apoptosis induced by 10 μM MGO + 3 μg/ml cisplatin. Fig. 3*B* shows that pretreatment with rottlerin also completely blocked ROS formation induced by 10 μM MGO + 3 μg/ml cisplatin treatment. As an additional control, 5 μM rottlerin was also examined for its ability to block apoptosis and ROS generation induced by 15 μg/ml cisplatin which it did (data not shown). Finally, to determine whether the mitogen-activated protein kinase pathway was critical to MGO + cisplatin-dependent cytotoxicity, apoptosis assays were performed using cells pretreated with 25 μM of the MEK inhibitor PD98059. As Fig. 3*C* demonstrates, MEK inhibition did not block apoptosis induced by MGO + cisplatin but instead enhanced it by 40%. Taken together these results indicate that cytotoxicity induced by MGO + cisplatin requires the activity of PKCδ but not the mitogen-activated protein kinase pathway.

MGO/Cisplatin-dependent Activation of PKCδ Is Not Dependent on NAC-inhibitable ROS—PKCδ has been shown to be important in the response of cells to oxidative and/or genotoxic stress (20, 21). Fig. 4*A* (*top panel*) demonstrates that treatment of cells with 10 μM MGO + 3 μg/ml cisplatin leads to a 4-fold increase in PKCδ activity at 60 min as measured by the ability of PKCδ to phosphorylate H1 histone. Western analysis of PKCδ immunoprecipitates (*middle panel*) showed that PKCδ autophosphorylation of serine 660 peaked between 60 and 90 min. Importantly, PKCδ mass was unaffected by MGO + cis-

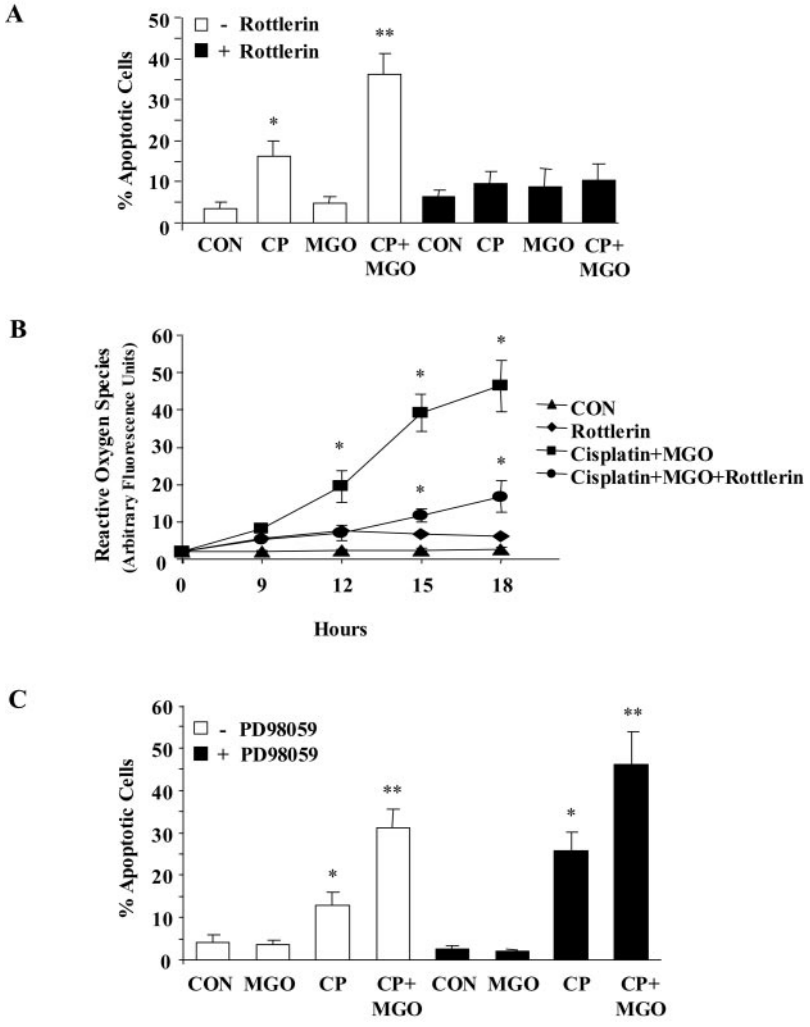

FIG. 3. **Inhibition of PKCδ with rottlerin blocks MGO/cisplatin-dependent apoptosis and ROS generation.** *A,* cells were treated for the times indicated with or without (*CON*) 3 μg/ml cisplatin (*CP*) and 10 μM MGO and/or 5 μM rottlerin. ROS accumulation was measured by flow cytometry using H_2DCF-DA staining. Results represent an average of three independent experiments ± S.E. Results significantly different from control at $\alpha = 0.05$ are indicated by *. Results significantly different from cisplatin (*CP*)-rottlerin at $\alpha = 0.05$ by a three-factor factorial assuming unequal variances are indicated by **. *B,* cells were treated for 18 h with or without (*CON*) 3 μg/ml cisplatin, 10 μM MGO, and/or 5 μM rottlerin. Apoptotic cell death was measured by flow cytometry using Hoechst and PI double staining. Results represent an average of three independent experiments ± S.E. Results significantly different from control at $\alpha = 0.05$ are indicated by *. *C,* cells were treated for 18 h with or without (*CON*) 3 μg/ml cisplatin, 10 μM MGO, and/or 25 μM PD98059. Apoptotic cell death was measured by flow cytometry using Hoechst and PI double staining. Results represent an average of three independent experiments ± S.E. Results significantly different from control at $\alpha = 0.05$ are indicated by *. Results significantly different from cisplatin (*CP*) −PD98059 at $\alpha = 0.05$ by a three-factor factorial assuming unequal variances are indicated by **.

platin treatment (*bottom panel*). Fig. 4*B* demonstrates that as expected pretreatment of cells with 5 μM rottlerin for 15 min blocked 10 μM MGO + 3 μg/ml cisplatin-induced PKCδ autophosphorylation. Rottlerin, however, did not block all actions of MGO + cisplatin leaving unaffected the increase in $p21^{Cip}$ mass induced by 10 μM MGO + 3 μg/ml cisplatin as measured by Western analysis between 0 and 3 h (Fig. 4*C*). Finally, Fig. 4*D* demonstrates that pretreatment of cells for 15 min with 10 mM NAC did not alter peak PKCδ kinase activity induced by MGO + cisplatin. At 60 min, 10 μM MGO increased PKCδ activity 25%, 3 μg/ml cisplatin increased PKCδ activity 2-fold, and 10 μM MGO + 3 μg/ml cisplatin increased PKCδ activity 4-fold. NAC pretreatment did not block this 4-fold effect. Taken together these results indicate that the activation of PKCδ induced by MGO + cisplatin is an early signal transduction event with peak activation occurring within 60 min of MGO + cisplatin addition to cells. In addition, this activation event is not dependent on NAC-inhibitable ROS. Importantly, PKCδ inhibition does not block all actions of MGO + cisplatin because the $p21^{Cip}$ mass increase was not affected. This finding suggests that signaling pathways activated by DNA damage are not regulated by PKCδ.

PKCδ Activates c-Abl in Response to MGO + Cisplatin—Oxidative stress activates c-Abl through a pathway that relies on PKCδ (40). To determine whether carbonyl stress in combination with cisplatin activated c-Abl, c-Abl kinase assays were performed. Fig. 5*A* shows that at 90 min 10 μM MGO + 3 μg/ml cisplatin led to a 4-fold increase in c-Abl tyrosine kinase activity. Neither 10 μM MGO nor 3 μg/ml cisplatin alone induced an increase in c-Abl activity (data not shown). Fig. 5*B* demonstrates that pretreatment of cells with 5 μM rottlerin for 15 min blocked by 75% 10 μM MGO + 3 μg/ml cisplatin-induced c-Abl kinase activity. Fig. 5*C* shows by Western analysis that 10 μM MGO + 3 μg/ml cisplatin treatment increased c-Abl:PKCδ association (*top panel*) and that rottlerin did not block formation of these complexes (*bottom panel*). As above, neither 10 μM MGO nor 3 μg/ml cisplatin alone induced c-Abl:PKCδ association (data not shown). To determine the impact of c-Abl inhibition on apoptosis induced by 10 μM MGO + 3 μg/ml cisplatin, flow cytometry was performed. Fig. 5*D* demonstrates that treatment of cells with 50 μM of the c-Abl inhibitor STI-571 (41) increased by 50% apoptosis induced by MGO + cisplatin at 18 h. Additionally, treatment of cells with the PIK-related kinase family inhibitor wortmannin (42) (1 μM) did not significantly change apoptosis induced by MGO + cisplatin. Finally, the impact of NAC and wortmannin on c-Abl kinase activity was examined. Fig. 5*E* shows that concurrent treatment of cells with 10 mM NAC blocked the ability of 10 μM MGO + 3 μg/ml cisplatin to activate c-Abl, whereas treatment with 1 μM wortmannin had no effect. Taken together these results indicate that MGO + cisplatin activate c-Abl and induce its association with PKCδ. Furthermore, inhibition of c-Abl increases the cytotoxicity of MGO + cisplatin implicating c-Abl as part of a cell survival pathway as opposed to one leading to cell death.

DISCUSSION

These data establish that MGO synergistically enhances cisplatin-induced apoptosis through a mechanism requiring acti-

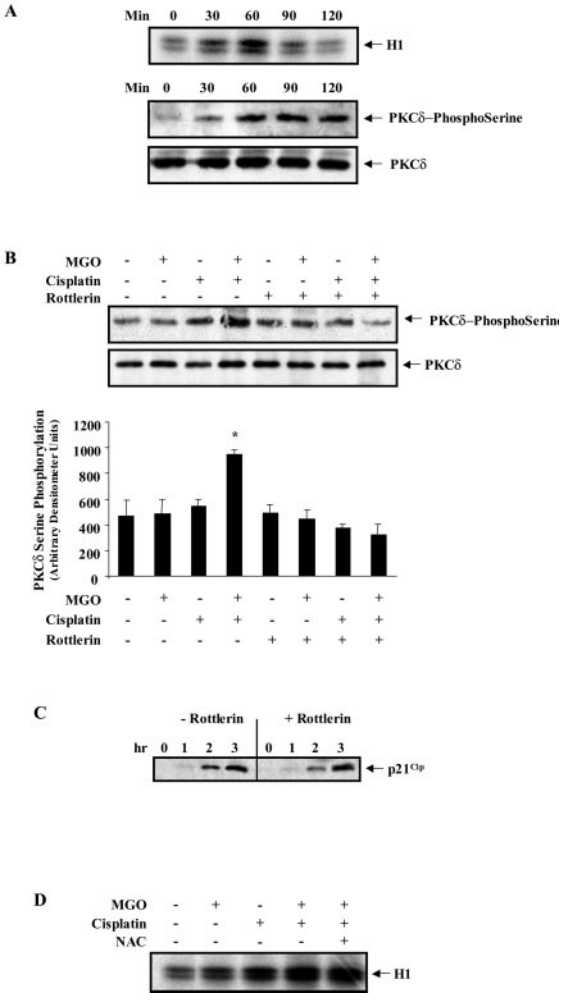

FIG. 4. **MGO/cisplatin-dependent activation of PKCδ is not dependent on NAC-inhibitable ROS.** *A, top panel,* cells were treated with 10 μM MGO + 3 μg/ml cisplatin for the times indicated, and PKCδ activity was measured in PKCδ immunoprecipitates using PKCδ kinase assays with histone 1 (*H1*) as a substrate. Results are representative of three independent experiments. *A, middle and bottom panels,* cells were treated as above, and PKCδ autophosphorylation on serine 660 (*middle*) and PKCδ mass (*bottom*) were measured in PKCδ immunoprecipitates by Western analysis using a phosphospecific PKC phosphoserine 660 antibody or a PKCδ antibody, respectively. Results are representative of three independent experiments. *B,* cells were treated for 60 min with 10 μM MGO, 3 μg/ml cisplatin, and/or 5 μM rottlerin as indicated. PKCδ autophosphorylation on serine 660 (*top panel*) and PKCδ mass (*middle panel*) were measured in PKCδ immunoprecipitates by Western analysis using a phosphospecific PKC phosphoserine 660 antibody or a PKCδ antibody, respectively. Results are representative of three independent experiments. Densitometry analysis of the *top panel* is shown as an average of three independent experiments ± S.E. in the *bottom panel,* and results significantly different from control at $\alpha = 0.05$ are indicated by *. *C,* cells were treated for the times indicated with 10 μM MGO + 3 μg/ml cisplatin with (+ rottlerin) or without (− rottlerin) 5 μM rottlerin, and the mass of $p21^{Cip}$ was measured by Western analysis in whole cell lysates using a $p21^{Cip}$ antibody. Results are representative of three independent experiments. *D,* cells were treated for 60 min with 10 μM MGO, 3 μg/ml cisplatin, and/or 10 mM NAC as indicated. PKCδ activity was measured in PKCδ immunoprecipitates using PKCδ kinase assays with histone 1 (*H1*) as a substrate. Results are representative of three independent experiments.

vation of PKCδ. Fig. 1*A* shows that cisplatin-dependent apoptosis was blocked by NAC and that NAC also prevented cisplatin-induced capsase-3 activation (Fig. 1*B*), intracellular ROS accumulation (Fig. 1*C*), and GSH loss (Fig. 1*D*). NAC, however, did not inhibit all actions of cisplatin in that cisplatin-dependent p53 expression was not altered. MGO synergized with cisplatin to induce apoptosis and intracellular ROS ac-

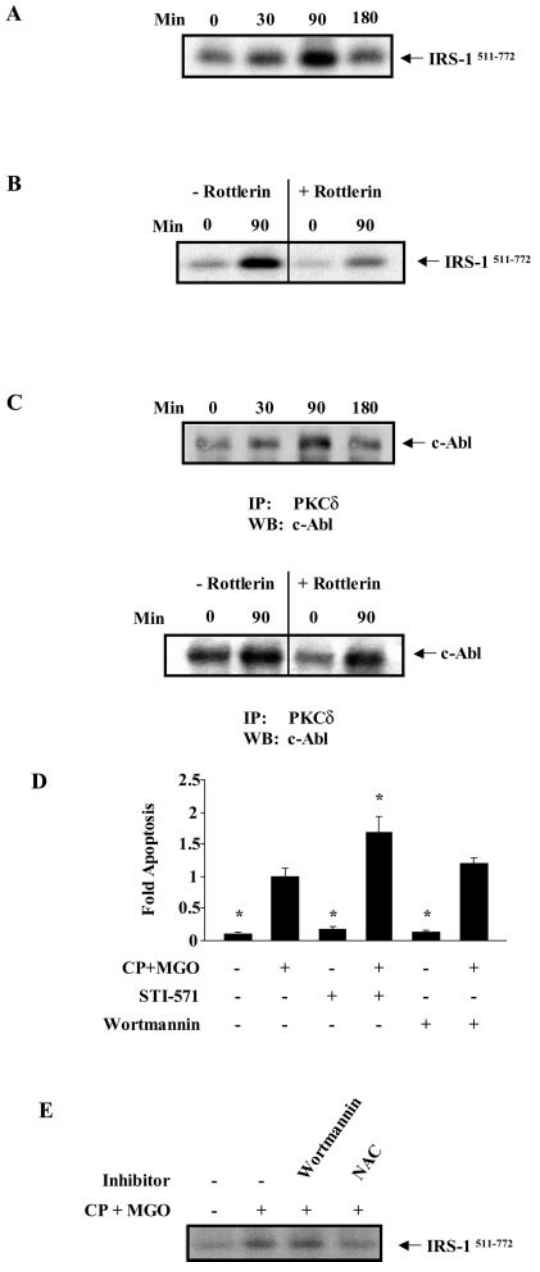

FIG. 5. **PKCδ activates c-Abl in response to MGO + cisplatin.** *A,* cells were treated with 3 μg/ml cisplatin + 10 μM MGO for the times indicated, and c-Abl activity was measured in c-Abl immunoprecipitates using c-Abl kinase assays with IRS-1-(511–772) as a substrate. Results are representative of three independent experiments. *B,* cells were treated for the times indicated with 10 μM MGO + 3 μg/ml cisplatin with (+ rottlerin) or without (− rottlerin) 5 μM rottlerin, and c-Abl activity was measured in c-Abl immunoprecipitates using c-Abl kinase assays with IRS-1-(511–772) as a substrate. Results are representative of three independent experiments. *C, top panel,* cells were treated as in *A,* and c-Abl mass was measured in PKCδ immunoprecipitates (IP) by Western analysis (WB). *C, bottom panel,* cells were treated as in *B* and c-Abl mass was measured in PKCδ immunoprecipitates (*IP*) by Western analysis (*WB*). Results are representative of three independent experiments. *D,* cells were treated for 18 h with (+) or without (−) 10 μM MGO + 3 μg/ml cisplatin (*CP*), 50 μM STI-571, and/or 1 μM wortmannin as indicated. Apoptotic cell death was measured by flow cytometry using Hoechst and PI double staining. Results represent an average of three independent experiments ± S.E. Results significantly different from cisplatin + MGO (+), STI-571 (−), and wortmannin (−) at $\alpha = 0.05$ are indicated by *. *E,* cells were treated for 90 min with (+) or without (−) 10 μM MGO + 3 μg/ml cisplatin (*CP*), 10 mM NAC, and/or 1 μM wortmannin as indicated. Activity of c-Abl was measured in c-Abl immunoprecipitates using c-Abl kinase assays with IRS-1-(511–772) as a substrate. Results are representative of three independent experiments.

cummulation (Fig. 2, *A–C*), doubling the expected additive effects of MGO + cisplatin. In turn, NAC blocked the ability of MGO + cisplatin to induce ROS accumulation and apoptosis (Fig. 2, *B* and *C*). Importantly, the PKCδ inhibitor rottlerin but not the MEK inhibitor PD98059 (Fig. 3) blocked MGO + cisplatin-induced apoptosis. MGO + cisplatin increased PKCδ activation by 4-fold between 60 and 90 min after MGO + cisplatin addition, whereas rottlerin blocked this effect (Fig. 4, *A* and *B*). Interestingly, rottlerin did not inhibit all actions of MGO + cisplatin in that MGO + cisplatin-dependent $p21^{Cip}$ expression was not altered (Fig. 4*C*). Additionally, NAC did not inhibit the ability of MGO + cisplatin to activate PKCδ (Fig. 4*D*). Finally, MGO + cisplatin induced c-Abl activation and c-Abl:PKCδ association. Use of the c-Abl inhibitor STI-571 increased MGO + cisplatin-dependent apoptosis by 50%. Taken together these data indicate that MGO synergistically enhances cisplatin-induced apoptosis through activation of PKCδ and that PKCδ is critical to both cell death and cell survival pathways.

Platinum-containing anti-neoplastic agents like cisplatin are needed in the treatment of advanced bladder cancer and metastatic ovarian and testicular cancers (11–13). Irreversible adverse reactions to platinum-based cancer drugs include nephrotoxicity and neurotoxicity. Furthermore, drug-related neurotoxicity is the major dosage-limiting toxicity of cisplatin (43). Because renal insufficiency and peripheral neuropathies are critical diabetic complications (22, 44), patients with diabetes are often unable to tolerate platinum-based anticancer therapies due to exacerbation of their pre-existing renal and neural complications (2–4). Studies examining the mechanism of action of cisplatin have implicated ROS and GSH as important modulators of cisplatin cytotoxicity (18). Our data support these findings in that pretreatment of cells with NAC blocks cisplatin-dependent caspase-3 activation and apoptosis by inhibiting intracellular ROS accumulation and maintaining intracellular GSH levels. Consistent with these findings is that conjugation of GSH to cisplatin appears to be an important mechanism by which cells eliminate cisplatin from their cytosol (45). Importantly, we found that NAC did not block all actions of cisplatin because the increased p53 mass induced by cisplatin between 1 and 6 h was not affected by addition of NAC. This was not unexpected because the cytotoxicity of cisplatin is thought to occur primarily through induction of DNA damage initially caused by cisplatin-DNA adducts (14), making the early signal transduction events in cisplatin action likely those that identify and attempt to repair damaged DNA. As previous studies have shown, cisplatin/DNA adducts trigger DNA mismatch repair enzymes (45) that then can activate p53 (39, 46). This induces increased $p21^{Cip}$ expression resulting in either G_1 or M arrest (47, 48). Failure to implement DNA repair eventually results in mitochondrial damage and release of apoptosome components that lead to terminal caspase activation. This later mitochondrial phase in the apoptotic process can be blocked by antioxidants and caspase inhibitors as we (Fig. 1) and others have shown (48).

Hyperglycemia and by-products of glucose metabolism like MGO are thought to play an essential role in the chronic complications of DM (1). One of the mechanisms by which this abnormal glucose metabolism is thought to impact the development of diabetic complications is through oxidative/carbonyl stress (1). Since both oxidative and carbonyl stress lead to reduced intracellular concentrations of antioxidants like GSH (1, 49), cells susceptible to oxidative damage from drugs that consume antioxidants in their action, detoxification and/or transmembrane transport would likely be more vulnerable to such damage in the diabetic patient who generally have lowered intracellular GSH (50). Our data support this idea because when MGO was combined with cisplatin, apoptosis and ROS generation were increased, and intracellular GSH was reduced. Surprisingly, however, these effects were synergistic leading to nearly a doubling of apoptosis and ROS generation when compared with the expected additive effects of these two compounds. Furthermore, we examined the monocytic cell line U937 that has been shown to be susceptible to hydrogen peroxide-induced oxidative stress (40), and we found that MGO + cisplatin induced synergistic cytotoxicity more than double the additive effects of MGO and cisplatin alone (data not shown). These results are likely explained by the fact that MGO and cisplatin work on different parts of the apoptosis cascade. Cisplatin, as noted above, is a DNA-damaging agent that activates $p21^{Cip}$ checkpoints through a p53-dependent mechanism. MGO, however, is an inducer of oxidative stress that appears to have its most important role in apoptosis during the mitochondrial phase (40). Our data support this because DNA damage-related events like $p21^{Cip}$ and p53 mass up-regulation were not affected by antioxidant pretreatments, whereas oxidative damage-related pathways like ROS generation and caspase activation were.

Activated PKCδ is increased in diabetic rats (51, 52), and elevations in PKC activity appear important to the development of diabetic complications like nephrotoxicity (22, 41, 53). One of the potential mechanisms by which PKCδ becomes activated in the diabetic patient is through an oxidative stress-dependent pathway. In fact, depletion of glutathione can activate PKCs (54). Recently, studies (19–21) have shown that hydrogen peroxide can activate PKCδ through a mechanism that appears to involve c-Abl-dependent tyrosine phosphorylation of PKCδ tyrosine 512 which then activates PKCδ independent of lipid cofactors. Here we show that MGO + cisplatin activates PKCδ but that PKCδ is responsible for the activation of c-Abl. In addition, we show that MGO + cisplatin increases c-Abl:PKCδ complex formation and that blockage of PKCδ activity with rottlerin neither inhibits MGO + cisplatin-dependent c-Abl:PKCδ complex formation nor reduces induction of increased $p21^{Cip}$ mass despite blocking MGO + cisplatin-dependent c-Abl activation. These results indicate that unlike the hydroxyl radical-dependent oxidative stress seen with hydrogen peroxide, c-Abl is not the initiating sensor/activator of apoptosis. This idea is supported because NAC did not block the ability of MGO + cisplatin to activate PKCδ. Although it was anticipated that NAC would prevent MGO + cisplatin-dependent apoptosis and ROS generation based on our findings in Fig. 1 and recently published work (19) concerning the importance of ROS in the mitochondrial phase of apoptosis, it was surprising to find that NAC did not block PKCδ activation because phorbol ester-independent activation of PKCδ is thought to work through a mechanism requiring ROS. The likely reason for this is that MGO is a reactive carbonyl, and reactive carbonyls are poorly quenched by NAC.

Finally, use of the c-Abl inhibitor STI-571 increased MGO + cisplatin-dependent apoptosis by 50%, whereas the PIK-related kinase family inhibitor wortmannin had no significant impact on cytotoxicity. These results are consistent with the potential role of c-Abl in DNA damage repair (48), and the data show that cisplatin itself is an inhibitor of PIK-related kinases like DNA-PK (55), making wortmannin inhibition redundant with cisplatin. NAC also blocked c-Abl activation. This finding was unexpected because NAC did not block PKCδ activation, and Fig. 5*B* shows that c-Abl activation is rottlerin-sensitive. This finding suggests that c-Abl activation relies both on PKCδ activity and on an oxidation response pathway. It also sepa-

rates c-Abl activation from events directly related to DNA damage like $p21^{Cip}$ and p53 mass up-regulation. In summary, MGO synergizes with cisplatin to induce apoptosis. The mechanism of this interaction appears to require PKCδ activation and PKCδ-dependent activation of c-Abl. Furthermore, whereas NAC-quenchable ROS are involved in the ability of MGO to increase the cytotoxicity of cisplatin, they appear important to its later stages, the mitochondrial phase. Activation of p53-dependent checkpoints like $p21^{Cip}$ apparently occur independent of MGO, PCKδ, and c-Abl and are likely induced by cisplatin-dependent DNA damage initially sensed by the PIK-related kinases.

REFERENCES

1. Baynes, J. W., and Thorpe, S. R. (1999) *Diabetes* **48,** 1–9
2. Stewart, D. J., Eapen, L., Hirte, W. E., Futter, N. G., Moors, D. E., Murphy, P. G., Irvine, A. H., Genest, P., McKay, D. E., Evans, W. K., Rasuli, P., Peterson, R. A., and Maroun, J. A. (1987) *J. Urol.* **138,** 302–305
3. Mollman, J. E., Glover, D. J., Hogan, W. M., and Furman, R. E. (1988) *Cancer* (*Phila.*) **61,** 2192–2195
4. Gogas, H., Shapiro, F., Aghajanian, C., Fennelly, D., Almadrones, L., Hoskins, W. J., and Spriggs, D. R. (1996) *Gynecol. Oncol.* **61,** 22–26
5. Poulson, J. (1997) *J. Pain Symptom Manage.* **13,** 339–346
6. The Diabetes Control and Complications Trial Research Group (1993) *N. Engl. J. Med.* **329,** 977–986
7. Thornalley, P. (1996) *Gen. Pharmacol.* **27,** 565–573
8. Thornalley, P. J., Hooper, N. I., Jennings, P. E., Florkowski, C. M., Jones, A. F., Lunec, J., and Barnett, A. H. (1989) *Diabetes Res. Clin. Pract.* **7,** 115–120
9. McLellan, A. C., Thornalley, P. J., Benn, J., and Sonksen, P. H. (1994) *Clin. Sci.* (*Lond.*) **87,** 21–29
10. Thornalley, P. J., Langborg, A., and Minhas, H. S. (1999) *Biochem. J.* **344,** 109–116
11. Ozols, R. F., and Young, R. C. (1991) *Semin. Oncol.* **18,** 222–232
12. Hartmann, J. T., Kanz, L., and Bokemeyer, C. (1999) *Drugs* **58,** 257–281
13. Witjes, J. A. (1997) *Drugs* **53,** 404–414
14. Chu, G. (1994) *J. Biol. Chem.* **269,** 787–790
15. Miyajima, A., Nakashima, J., Tachibana, M., Nakamura, K., Hayakawa, M., and Murai, M. (1999) *Jpn. J. Cancer Res.* **90,** 565–570
16. Godwin, A. K., Meister, A., O'Dwyer, P. J., Huang, C. S., Hamilton, T. C., and Anderson, M. E. (1992) *Proc. Natl. Acad. Sci. U. S. A.* **89,** 3070–3074
17. Sheikh-Hamad, D., Timmins, K., and Jalali, Z. (1997) *J. Am. Soc. Nephrol.* **8,** 1640–1644
18. Miyajima, A., Nakashima, J., Yoshioka, K., Tachibana, M., Tazaki, H., and Murai, M. (1997) *Br. J. Cancer* **76,** 206–210
19. Sun, X., Wu, F., Datta, B., Kharbanda, S., and Kufe, D. (2000) *J. Biol. Chem.* **275,** 7470–7473
20. Yuan, Z. M., Utsugisawa, T., Ishiko, T., Nakada, S., Huang, Y., Kharbanda, S., Weichselbaum, R., and Kufe, D. (1998) *Oncogene* **16,** 1643–1648
21. Konishi, H., Tanaka, M., Takemura, Y., Matsuzaki, H., Ono, Y., Kikkawa, U., and Nishizuka, Y. (1997) *Proc. Natl. Acad. Sci. U. S. A.* **94,** 11233–11237
22. Ishii, H., Koya, D., and King, G. L. (1998) *J. Mol. Med.* **76,** 21–31
23. Nishizuka, Y. (1984) *Nature* **308,** 693–698
24. Mellor, H., and Parker, P. J. (1998) *Biochem. J.* **332,** 281–292
25. Newton, A. C. (1995) *J. Biol. Chem.* **270,** 28495–28498
26. Ron, D., and Kazanietz, M. G. (1999) *FASEB J.* **13,** 1658–1676
27. Parekh, D. B., Ziegler, W., and Parker, P. J. (2000) *EMBO J.* **19,** 496–503
28. Gschwendt, M. (1999) *Eur. J. Biochem.* **259,** 555–564
29. Gschwendt, M., Muller, H. J., Kielbassa, K., Zang, R., Kittstein, W., Rincke, G., and Marks, F. (1994) *Biochem. Biophys. Res. Commun.* **199,** 93–98
30. Wang, X., Martindale, J. L., and Holbrook, N. J. (2000) *J. Biol. Chem.* **275,** 39435–39443
31. Isonishi, S., Andrews, P. A., and Howell, S. B. (1990) *J. Biol. Chem.* **265,** 3623–3627
32. Basu, A., and Akkaraju, G. R. (1999) *Biochemistry* **38,** 4245–4251
33. Godbout, J. P., Cengel, K. A., Cheng, S. L., Minshall, C., Kelley, K. W., and Freund, G. G. (1999) *Cell. Signal.* **11,** 15–23
34. Scaffidi, C., Fulda, S., Srinivasan, A., Friesen, C., Li, F., Tomaselli, K. J., Debatin, K. M., Krammer, P. H., and Peter, M. E. (1998) *EMBO J.* **17,** 1675–1687
35. Nicholson, D. W., Ali, A., Thornberry, N. A., Vaillancourt, J. P., Ding, C. K., Gallant, M., Gareau, Y., Griffin, P. R., Labelle, M., Lazebnik, Y. A., Munday, N. A., Raju, S. M., Smulson, M. E., Yamin, T.-T., Yu, V. L., and Miller, D. K. (1995) *Nature* **376,** 37–43
36. Sanchez, A., Alvarez, A. M., Benito, M., and Fabregat, I. (1996) *J. Biol. Chem.* **271,** 7416–7422
37. Griffith, O. W. (1980) *Anal. Biochem.* **106,** 207–212
38. Cengel, K. A., and Freund, G. G. (1999) *J. Biol. Chem.* **274,** 27969–27974
39. Yuan, Z. M., Huang, Y., Fan, M. M., Sawyers, C., Kharbanda, S., and Kufe, D. (1996) *J. Biol. Chem.* **271,** 26457–26460
40. Kumar, S., Bharti, A., Mishra, N. C., Raina, D., Kharband, S., Saxena, S., and Kufe, D. (2001) *J. Biol. Chem.* **276,** 17281–17285
41. Buchdunger, E., Zimmermann, J., Mett, H., Meyer, T., Muller, M., Druker, B. J., and Lydon, N. B. (1996) *Cancer Res.* **56,** 100–104
42. Chan, D. W., Son, S. C., Block, W., Ye, R., Khanna, K. K., Wold, M. S., Douglas, P., Goodarzi, A. A., Pelley, J., Taya, Y., Lavin, M. F., and Lees-Miller, S. P. (2000) *J. Biol. Chem.* **275,** 803–810
43. Siftin, D. W. (ed) (2001) *Physicians Desk Reference,* pp. 1055–1057, 55th Ed, Medical Economics Publishing, Inc., Montvale, NJ
44. Ha, H., and Kim, K. H. (1999) *Diabetes Res. Clin. Pract.* **45,** 147–151
45. Ishikawa, T., and Ali-Osman, F. (1993) *J. Biol. Chem.* **268,** 20116–20125
46. Sionov, R. V., Moallem, E., Berger, M., Kazaz, A., Gerlitz, O., Ben-Neriah, Y., Oren, M., and Haupt, Y. (1999) *J. Biol. Chem.* **274,** 8371–8374
47. Levine, A. J. (1997) *Cell* **88,** 323–331
48. Rich, T., Allen, R. L., and Wyllie, A. H. (2000) *Nature* **407,** 777–783
49. Thornalley, P. J., McLellan, A. C., Lo, T. W., Benn, J., and Sonksen, P. H. (1996) *Clin. Sci.* (*Lond.*) **91,** 575–582
50. Yoshida, K., Hirokawa, J., Tagami, S., Kawakami, Y., Urata, Y., and Kondo, T. (1995) *Diabetologia* **38,** 201–210
51. Kapor-Drezgic, J., Zhou, X., Babazono, T., Dlugosz, J. A., Hohman, T., and Whiteside, C. (1999) *J. Am. Soc. Nephrol.* **10,** 1193–1203
52. Igarashi, M., Wakasaki, H., Takahara, N., Ishii, H., Jiang, Z. Y., Yamauchi, T., Kuboki, K., Meier, M., Rhodes, C. J., and King, G. L. (1999) *J. Clin. Invest.* **103,** 185–195
53. Ikeda, S., Fukuzaki, A., Kaneto, H., Ishidoya, S., and Orikasa, S. (1999) *Int. J. Urol.* **6,** 245–250
54. Domenicotti, C., Paola, D., Vitali, A., Nitti, M., d'Abramo, C., Cottalasso, D., Maloberti, G., Biasi, F., Poli, G., Chiarpotto, E., Marinari, U. M., and Pronzato, M. A. (2000) *Free Radic. Biol. Med.* **229,** 1280–1290
55. Turchi, J. J., Patrick, S. M., and Henkels, K. M. (1997) *Biochemistry* **36,** 7586–7593